

Self-assembly of the gyroid cubic mesophase: lattice-Boltzmann simulation

Nelido Gonzalez-Segredo () and Peter V. Coveney ()

Centre for Computational Science, Department of Chemistry, University College London
- 20 Gordon Street, London WC1H 0AJ, United Kingdom.

PACS. 61.30.St { Lyotropic phases.

PACS. 61.20.Lc { Time-dependent properties; relaxation.

Abstract. { We present the first simulations of the self-assembly kinetics of the gyroid cubic mesophase using a Boltzmann transport method. No macroscopic parameters are included in the model and three-dimensional hydrodynamics is emergent from the microscopic conservation laws. The self-assembly arises from local inter-particle interactions in an initially homogeneous, phase-segregating binary fluid with dispersed amphiphile. The mixture evolves in discrete time according to the dynamics of a set of coupled Boltzmann-BGK equations on a lattice. We observe a transient microemulsion phase during self-assembly, the structure function peaks and direct-space imaging unequivocally identifies the gyroid at later times. For larger lattices, highly ordered subdomains are separated by grain boundaries. Relaxation towards the ordered equilibrium structure is very slow compared to the diffusive and microemulsion-assembly transients, the structure function oscillating in time due to a combination of Marangoni effects and long-time-scale defect dynamics.

Block copolymer melts or dispersions, and homopolymer-block copolymer blends are examples of systems that self-assemble into regular, liquid-crystalline structures when subjected to the appropriate temperature or pressure quenches [1,2,3,4]. These structures, called mesophases due to their features being intermediate between those of a solid and a liquid, are also found in fluid mixtures of a surfactant in a solvent, binary immiscible fluids containing a third, amphiphilic phase, and lipidic biological systems [1,5]. They all form due to the competing attraction-repulsion mechanism between the species. The morphology of these mesophases are defined by the spatial location where most of the amphiphile concentrates, forming multi- or mono-layer sheets of self-assembled amphiphile. Common equilibrium mesophases include lamellae, hexagonal columnar arrays, and the primitive "P", diamond "D" and gyroid "G" triply periodic minimal surfaces [1,2].

Simulation approaches to the dynamics of mesophase formation have been hitherto based on Monte Carlo [12], Brownian dynamics [10], dissipative particle dynamics [9,10,11], Langevin diffusion equation [7,8] and molecular dynamics methods [13]. In Langevin-diffusion methods, mass currents arise from chemical potential gradients, computed in turn from equilibrium free

() n.gonzalez-segredo@ucl.ac.uk

() p.v.coveney@ucl.ac.uk

energies. Much of the published work is based on Ginzburg-Landau expansions for the latter, assuming that all surfactant is adsorbed as a continuum on the self-assembled sheets, incorporating white noise and excluding hydrodynamics [7]. More recently, extensions appeared including hydrodynamics and free energies explicitly calculated for the amphiphile, modelled as Gaussian bead-spring chains in a mean-field environment [8]. Dissipative particle dynamics (DPD) methods also model the amphiphile as bead-spring chains, yet the beads as well as the particles constituting the fluid species enter in the model as truly mesoscopic entities experiencing conservative, dissipative and stochastic forces. In DPD, space is continuous and hydrodynamics is emergent from the mesodynamics. The presence of hydrodynamics is an important feature in modelling the nonequilibrium pathways of mesophase self-assembly and the possible metastable states they can lead to, but is absent in Monte Carlo [12] and Brownian dynamics [10] methods.

In this work we use a hydrodynamically correct lattice-Boltzmann model of amphiphilic fluids [4] to simulate the self-assembly of a liquid crystalline, double gyroid cubic phase from a randomly mixed initial binary immiscible fluid (say, of "oil" or "red", and "water" or "blue") with an amphiphilic species dispersed in it. The model, which is an extension of a modified Shan-Chen model for immiscible fluids [4], does not require the existence of a thermodynamic potential describing the local equilibria and a phase transition; rather, self-assembly arises as an emergent property of the microscopic interactions between the species. The dynamics is obtained by solving a set of coupled Boltzmann-BGK transport equations on a spatial lattice in discrete time steps with a discrete set of microscopic velocities; the scheme is known as the lattice-Boltzmann (LB) BGK method and has proved useful for single- and multi-phase flow modelling during the last decade [15]. At each time step, the probability density evolved by each LB equation is advected to nearest neighbours and modified by molecular collisions, which are local and conserve mass and momentum. A single time parameter controls relaxation in the collision term for all microscopic speeds, and in our model there is no stochastic noise present other than in the amphiphile dynamics. The mass density defines fluid elements on each lattice node which can be mapped onto experimental scales that are intermediate with respect to molecular and macroscopic lengths and times. Immiscible fluid behaviour is incorporated via scalar inter-particle forces of a mean-field form limited to nearest neighbours. The force enters in the hydrodynamics by modifying the local macroscopic velocity of the whole fluid and hence the local Maxwellian to which each species relaxes. For the correct lattice symmetry, and in the limits of low Mach numbers and large length and time scales, the Navier-Stokes equations for incompressible flow hold in the bulk of each fluid phase. The model also leads to the growth exponents and dynamical self-similarity observed in binary immiscible spinodal decomposition experiments [16]. A density of amphiphile is evolved by an additional coupled LB equation, and the bipolar, surfactant molecules are modelled as dipole vectors moving between the nodes of the lattice. Their orientations vary continuously and relax towards a Gaussian canonical equilibrium which minimises the interaction energy between the local dipole and mean fields generated by their nearest neighbours. The evolution of the surfactant density is also coupled to that of the other species [14].

The initial condition in our simulations is a random dispersion of surfactant in a random mixture of equal amounts of oil and water. The maximum values chosen for the (uniformly distributed) random densities were 0.70 for oil or water and 0.40;0.60;0.90 $n^{(0)s}$ for the surfactant. These, as well as all magnitudes and parameters in the model, are in lattice units. All relaxation times were set to 1.0, the thermal noise parameter for dipolar relaxation was set to 10.0, and the parameters controlling the strength of the inter-species forces were set to $g_{br} = 0.08$, $g_{bs} = 0.006$ and $g_{sr} = 0.003$. We employed periodic boundary conditions on cubic lattices of 64^3 , 128^3 and 256^3 nodes, the latter two initially being required to check

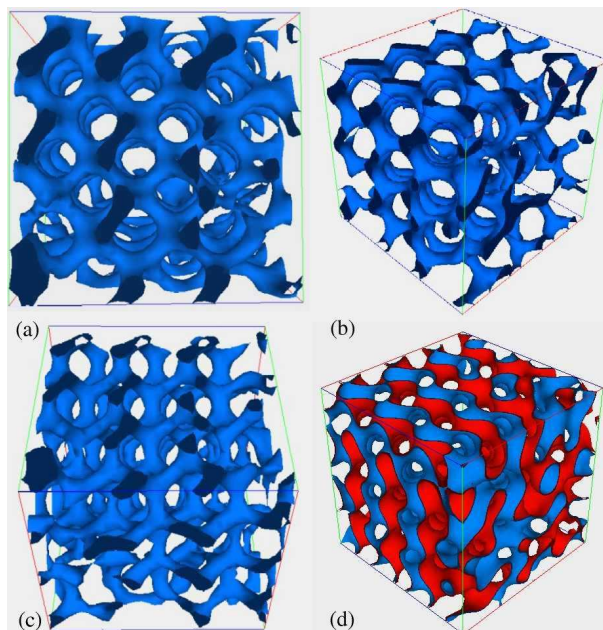


Fig. 1 { Isosurfaces of the order parameter $\phi(x)$ for a surfactant density of $n^{(0)s} = 0.60$ at time step $t = 15000$ in a highly ordered 33^3 subdomain of a 128^3 lattice. Panels (a), (b), and (c) display the $\phi = 0.40$, high-density isosurface viewed along the (100) , $(1\bar{1}\bar{1})$ and (110) directions, respectively, and colour is arbitrary. Panel (d) shows the oil-water interface ($\phi = 0$) of the same lattice subdomain along the direction $(1\bar{1}\bar{1})$, where between three and four units cells t laterally in the subdomain. Red and blue denote the two immiscible species.

that finite size effects were absent. The choices made of densities and parameters was based on previous tests searching for regimes of oil-water immiscibility (i.e., below the spinodal) for which, within the computing time and resources available, phase segregation was sufficiently fast while flows were dominated by hydrodynamics and surface tension as opposed to diffusion.

We are interested in studying the nonequilibrium pathways that follow from the initial condition, for which we track the evolution of mass densities via direct-space imaging and analysis of the structure function. Defining a scalar order parameter, $\phi(x)$, at a particular time step as the oil density minus the water density, the oil-water structure function, $S(k)$, is the Fourier transform of the spatial auto-correlation function for the fluctuations of $\phi(x)$ around its lattice average, proportional to the intensities probed in scattering techniques widely used in the analysis of mesophase structure; the spherically averaged structure function, $\bar{S}(k)$, is the average of $S(k)$ in a shell of radius $k = |\mathbf{k}|$ and thickness one lattice unit, corresponding to the contribution of structures of size $L = 2\pi/k$.

Figure 1 shows isosurfaces of the order parameter at time step $t = 15000$ in a 33^3 subdomain of a 128^3 lattice for an initial surfactant density initially distributed up to $n^{(0)s} = 0.60$. We display three viewpoints of the isosurface $\phi = 0.40$ (in lattice units), corresponding to a water-in-oil, "rod-like" scenario where water is a minority phase and oil is in excess. Whereas on 64^3 (or smaller) lattices, the liquid crystalline structure uniformly pervades the simulation cell, on 128^3 (or larger) lattices there are some imperfections present, more prevalent

as the lattice size is increased, resulting in liquid crystalline subdomains with slightly varying orientations between which exist domain boundaries | "defects". Globally, however, the $\epsilon > 0$ (excess) isosurfaces form interweaving, chirally symmetric, three-fold coordinated, bicontinuous lattices.

The resemblance of the simulated structures in Fig. 1 to transmission electron microtomography (EMT) images of the gyroid "G" cubic morphology is evident [4]. The lattice resolution is insufficient to detect multiple peak fingerprints in plots of $S(k)$, as observed experimentally with SAXS techniques [3,4]. However, its unaveraged counterpart (Fig. 2) shows complete agreement of ratios of reciprocal vector moduli with those observed in diffraction patterns of the gyroid [4], which, in addition to visual (direct space) inspection of the unit cell, leads to unequivocal identification. EMT images and experimental self-assembly times of the gyroid phase allows us to broadly associate a length and time scale to our LB dynamics, e.g. the systems in [4,17] require resolutions to be 2.3 nm per LB-lattice unit and 10 s up to 40 ms per LB time step.

Higher values than $n^{(0)s} = 0.60$ also produce gyroid structures at late times, whereas there is gradual loss of long-range ordering for $n^{(0)s} < 0.40$, leading to a molten gyroid phase. At $n^{(0)s} = 0.40$, the late-time structure becomes a sponge (microemulsion), isotropic and of short-range order, for which $S(k)$ is similar to that shown in Fig. 2, top row. Although the observation of gyroid-related morphologies has earlier been claimed in Langevin-diffusion [8] and DPD [9] methods, the evidence was purely pictorial and not comprehensive | in fact, the structures more closely resemble molten gyroid states.

Figure 3 shows the time evolution of the spherically averaged structure function for the $n^{(0)s} = 0.60$ gyroid case and wavenumbers corresponding to average domain sizes in $6.4 < L < 64$. Note three characteristic features of the curves: there are oscillations, decay (for $k < 0.83$ and $k > 1.1$, the latter not shown), and growth (for $0.88 < k < 1.0$ or $6.1 < L < 7.1$, close to the average domain size value). Modes of $k > 1.3$ ($L < 4.7$) decay fast enough ($S(k) < 0.1$ for $t = 1000$) that they do not contribute to the structure. The analogue curves for the $n^{(0)s} = 0.40$ case, leading to a sponge phase, exhibit similar oscillations, albeit of longer period. The fact that there are two types of temporal evolution, corresponding to increasing and decreasing modes, is a reflection of a phase segregation process still taking place. In the course of time, more domains accumulate in the $0.88 < k < 1.0$ range; we discard increasing interface steepness as another contributing factor to this since oil/water diffusion is negligible in this regime.

Direct-space observation of the interface ($\epsilon = 0$) superimposed on surfactant density maps for a series of time slices allows us to ascribe the oscillations that mainly affect the growing modes to "self-sustained" Marangoni effects. These are caused by collective and inhomogeneous amphiphile adsorption and desorption to and from the (periodically modulated) interface, a region of high surfactant density. This permits us to set a time scale of between 100 to 500 time steps during which interfacial surfactant from regions of high density diffuses towards an adjacent interface (also with adsorbed surfactant), effectively forming a bridge between the two sheets. If the interfaces belong to boundary, inter-domain regions, where the global translational symmetry is broken, defects form, change shape and annihilate on the same time scale. Perusal of Fig. 2 confirms that the smallest period of the oscillations is not dissimilar to such a time scale. The frequency spectrum of the time evolution of $S(k)$ gives a rich structure of peaks with a decaying envelope, higher-frequency modes becoming excited as the surfactant concentration increases.

Direct-space observation also shows an essential feature of the mesophase dynamics: each unit cell in the gyroid wanders in time about a fixed spatial position, whereas for the sponge the interface shows nonperiodic displacements. In other words, the temporal average of the

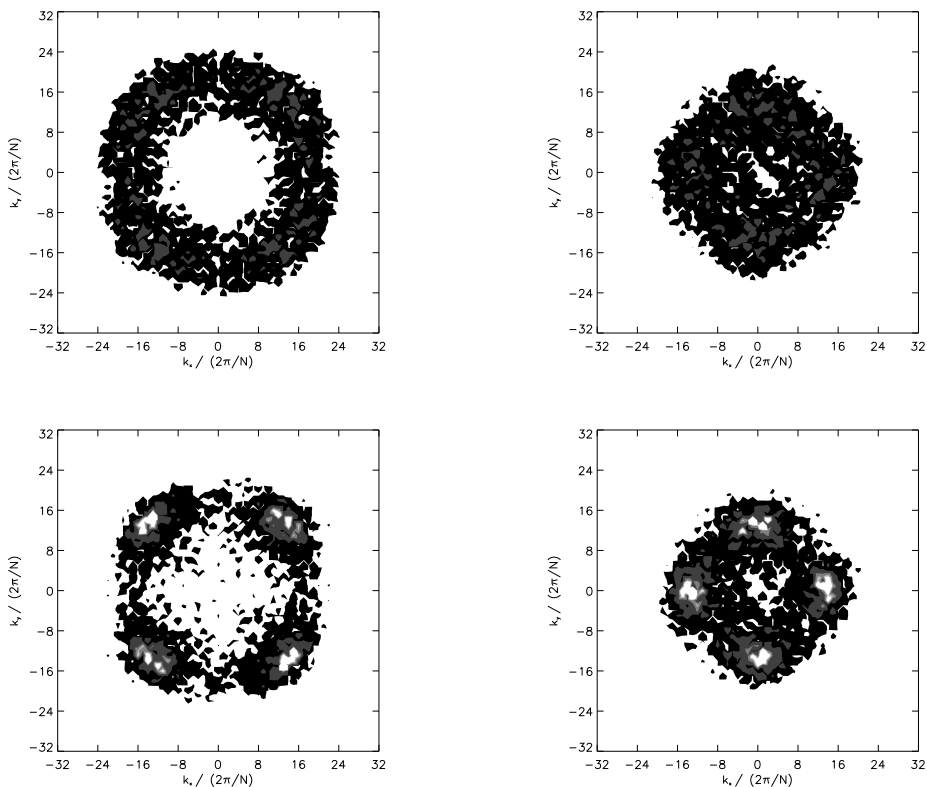


Fig. 2 (Temporal evolution of $(k_x; k_y)$ slices of the structure function viewed along the (100) direction. The grid is the same of Fig. 1. Left and right columns show slices at $k_z = (2\pi/N) = 0; 14$, respectively, where $N = 128$ is the lattice lateral size. Rows from top to bottom correspond to time steps $t = 500$ and 15000 , respectively. Contours denote intensities $S = 1; 50$ and 100 , where lighter shades denote higher intensities. The spherical shell structures in the top row indicate the presence of a sponge (microemulsion) phase, which becomes anisotropic at later times. In lattice units.

displacement is zero for a gyroid's unit cell and non-zero for an interface element in the sponge phase. Displacements are small in the former: they are not larger than ca. 20% of the unit cell size and are in-phase with those of the unit cells belonging to the local, defect-delimited subdomain. We therefore expect the gyroid structure to be stable, i.e. the dynamics would relax to it for late times.

Temporal oscillations in the structure function of sponge phases have been reported previously by Gompper & Hennes via a stochastic Langevin diffusion equation method with hydrodynamics, based on a Ginzburg-Landau free energy [18]. This approach does not explicitly consider an order parameter for the amphiphile since it assumes that amphiphile relaxation is fast compared to that of the oil-water order parameter. The oscillations reported therein range from overdamped to underdamped depending on the wavenumber, and their frequency spectrum shows a single peak at finite frequency. This is in contradistinction to our finding

of multiple-peak spectra, which we ascribe to the absence in that model of scalar or vector degrees of freedom for the amphiphile. In fact, Gompper & Hennes put forward a linearised Navier-Stokes model for Poiseuille flow wherein oscillations arise due to incompressibility competing with pressure gradients. Our LB method reproduces the same linearised, incompressible Navier-Stokes dynamics away from interfaces for the quiescent flows we observe, and, despite this, we obtain multiple-peak spectra. In addition, since stochastic sources are not present in the oil/water evolution, they cannot account for this spectral multiplicity. While it is true that randomness in the adsorbed surfactant directors may effectively reduce amphiphile adsorption strength, this effect is negligible compared to surfactant diffusion currents, facilitated by gradients of $\langle \chi \rangle$ from nearby interfaces.

Since the systems we simulate are dissipative and isolated (there is no mass or momentum exchange with external sources), oscillations are bound to die out at sufficiently late times. We observe interfacial widths to have reached their minimum (and hence interfacial tension its maximum) at about time step 1000, at which time the structure has a sponge-like morphology. Then the structure undergoes slow relaxation on a time scale which is $O(10^4)$. We observe the pathway to equilibration to be a slow process dominated by currents created by surface tension and Marangoni effects acting on similar time scales. A "free energy leading the way" towards the equilibrium morphology might be less useful than a correct mesodynamics, and even bias the evolution; methods which are intrinsically mesoscopic bottom-up such as ours and DPD are better suited. From DPD simulations of copolymer melts [9], Groot & Madden found that melts of symmetric amphiphile led to lamellar phases, whereas a gyroid-like structure appeared only for asymmetric amphiphile as a transient phase precursor to a hexagonal columnar phase. Our results are in contradistinction to these: although our amphiphiles are symmetric, the gyroids we find are stable.

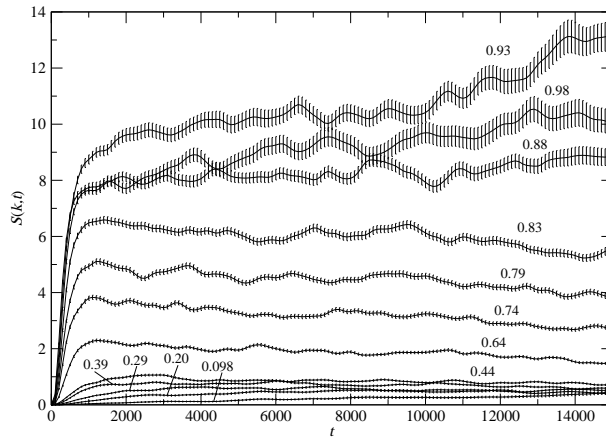


Fig. 3 { Temporal evolution of the spherically averaged structure function and its error (one standard deviation uncertainty in the average), for the wavenumbers indicated next to each curve. The fluid is the same as in Fig. 1. All quantities are in lattice units.

Finally, our reproduction of periodically modulated mesostructures rebuts claims that a necessary condition for their self-assembly is a disparity in the ranges of interaction of the competing morphogenic mechanisms, namely, short range versus long range [6]. Unlike other mesoscopic approaches such as DPD, ours is strictly local, being based on nearest neighbour interactions on a lattice.

The simulation of the gyroid cubic phase reported here highlights the richness of our

model's parameter space. Our LB model represents a kinetically and hydrodynamically correct, bottom-up, mesoscale description of the generic behavior of amphiphilic fluids, which is also algorithmically simple and extremely computationally efficient on massively parallel platforms [19]. Natural extensions of this work include the search for regimes leading to equilibrium mesophases of varied symmetries, the study of shear-induced symmetry transitions and the analysis of defect dynamics in large scale simulations. Computational steering tools should prove invaluable in these respects [20].

Access to supercomputer resources was provided by the UK EPSRC under grants GR/M 56234 and RealityGrid GR/R 67699.

REFERENCES

- [1] Seddon J. M. and Templer R. H., *Handbook of Biological Physics*, edited by R. Lipowsky and E. Sackmann, Vol. 1 (Elsevier Science B.V., Amsterdam) 1995, p. 97.
- [2] Klinowsky J., McKay A. L. and Terrones H., *Phil. Trans. R. Soc. Lond. A*, 354 (1996) 1975.
- [3] Laurer J. H., Hajduk D. A., Fung J. C., Sedat J. W., Smith S. D., Gruner S. M. and Agard D. A., Spontak R. J., *Macromolecules*, 30 (1997) 3938.
- [4] Hajduk D. A., Harper P. E., Gruner S. M., Honeker C. C., Kim G. and Thomas E. L., *Macromolecules*, 27 (1994) 4063.
- [5] Luzzati V., Vargas R., Mariani P., Gulik A. and Delacroix H. J., *Mol. Biol.*, 229 (1993) 540; Rummel G., Hardmeyer A., Widmer C., Chiu M. L., Nollert P., Locher K. P., Pedruzzi I., Landau E. M. and Rosenbusch, J. P., *J. Struct. Biol.*, 121 (1998) 82.
- [6] Seul M. and Andelman D., *Science*, 267 (1995) 476.
- [7] Nonomura M. and Ohta T., *J. Phys.: Condens. Matter*, 13 (2001) 9089; Imai M., Saeki A., Teramoto T., Kawaguchi A., Nakaya K., Kato T. and Ito K., *J. Chem. Phys.*, 115 (2001) 10525; Qi S. and Wang Z.-G., *Phys. Rev. E*, 55 (1997) 1682.
- [8] Zvelindovsky A. V., Sevink G. J. A. and Fraaije J. G. E. M., *Phys. Rev. E*, 62 (2000) R3063; van Vlimmeren B. A. C., Maurits N. M., Zvelindovsky A. V., Sevink G. J. A. and Fraaije J. G. E. M., *Macromolecules*, 32 (1999) 646.
- [9] Groot R. D. and Madden T. J., *J. Chem. Phys.*, 108 (1998) 8713.
- [10] Groot R. D., Madden T. J. and Tildesley D. J., *J. Chem. Phys.*, 110 (1999) 9739.
- [11] Prinsen P., Warren P. B. and Michels M. A. J., *Phys. Rev. Lett.*, 89 (2002) 148302.
- [12] Doter T. and Hatano A., *J. Chem. Phys.*, 105 (1996) 8413; Pakula T., Karatasos K., Anastasiadis S. H. and Fytas G., *Macromolecules*, 30 (1997) 8463.
- [13] Marrink S.-J. and Tieleman D. P., *J. Am. Chem. Soc.*, 123 (2001) 12383.
- [14] Chen H., Boghosian B. M., Coveney P. V. and Nekovee M., *Proc. Roy. Soc. Lond. A*, 456 (2000) 2043; Nekovee M., Coveney P. V., Chen H. and Boghosian, B. M., *Phys. Rev. E*, 62 (2000) 8282.
- [15] Succi S., *The lattice-Boltzmann equation for fluid dynamics and beyond* (Oxford University Press, Oxford) 2001.
- [16] Gonzalez-Segredo N., Nekovee M. and Coveney P. V., *Phys. Rev. E*, 67 (2003) 046304.
- [17] Squires A. M., Templer R. H., Seddon J. M., Woenckhaus J., Winter R., Finet S. and Theyencheri N., *Langmuir*, 18 (2002) 7384.
- [18] Gompper G. and Hennes M., *J. Phys. II France*, 4 (1994) 1375.
- [19] Love P. J., Nekovee M., Coveney P. V., Chin J., Gonzalez-Segredo N. and Martin J. M. R., *Comp. Phys. Commun.*, 153 (2003) 340.
- [20] URL: <http://www.RealityGrid.org>; Chin J., Harting J., Jha S., Coveney P. V., Porter A. R. and Pickles S. M., *Contemporary Physics*, 44 (2003) 417.